The Cosmic Ray Energetics and Mass (CREAM) Experiment Timing Charge Detector

J. J. Beatty [a*], H. S. Ahn [b], P. S. Allison [a], M. J. Choi [c], N. Conklin [a], S. Coutu [a], M. A. DuVernois [d], O. Ganel [b], S. Jaminion [a], M.H. Lee [b], L. Lutz [b], P. S. Marrocchesi [e], S. Minnick [a], S. I. Mognet [a], K. Min [f], S. Nutter [g], H. Park h, I.H. Park [c], K. Petska [a], E. Schindhelm [d], E.S. Seo [b], S. Swordy [k], J. Wu [b], and J. Yang [c]

[a] Departments of Physics and of Astronomy & Astrophysics, Penn State;
[b] Institute for Physical Science and Technology, University of Maryland;
[c] Department of Physics, Ewha Womans University, Korea;
[d] School of Physics and Astronomy, University of Minnesota;
[e] Department of Physics, University of Siena, and INFN;
[f] Department of Physics, Korea Advanced Institute of Science and Technology
[g] Department of Physics and Geology, Northern Kentucky University;
[h] Department of Physics, Kyungpook National University, Korea
[k] Enrico Fermi Institute and Department of Physics, The University of Chicago

ABSTRACT

The cosmic ray all-particle spectrum has a small steepening of its spectral slope, or 'knee', near 10^{15} eV. Changes in the nuclear composition of cosmic rays may be associated with the knee and provide clues concerning the origin of the spectral change. An ultra-long duration balloon experiment, Cosmic Ray Energetics and Mass (CREAM), is being constructed to measure cosmic ray elemental spectra at energies just below the knee to look for evidence of changes in composition. CREAM employs a thin calorimeter and transition radiation detector to provide multiple measures of the particle energy. A novel technique, the timing charge detector, is used to identify the charge of the incident primary cosmic ray in the presence of the albedo particles generated by interactions in the calorimeter.

Keywords: cosmic rays, scintillation counters, Calorimetry, balloon instrumentation

1. SCIENTIFIC CONTEXT OF THE CREAM EXPERIMENT

Cosmic rays are high-energy charged particles, mostly atomic nuclei, accelerated in a variety of astrophysical environments. Cosmic rays have been observed over a wide range of energies. At energies below about 10^9 electron-volts (eV), the flux of cosmic rays varies significantly with the solar cycle, due both to particle acceleration within the solar system and to the reduction in the flux of particles from outside sources due to plasma phenomena within the heliosphere. Above 10^9 eV most particles are of extrasolar origin. Shock acceleration in supernova remnants is believed to be the dominant mechanism for production of cosmic rays up to about 10^{15} eV. Cosmic rays have been observed with energies above 10^{20} eV. The origin of the highest energy cosmic rays is likely to be extragalactic.

At energies above about 10^{14} eV, the cosmic ray flux is low and space-based direct measurements of cosmic rays become difficult due to the need for extremely large areas and long exposures. Indirect measurements must be used above this energy, making use of the Earth's atmosphere as the target. Figure 1 shows the cosmic ray all-particle spectrum measured using a combination of different techniques. The spectrum is remarkably smooth over 11 orders of magnitude in energy, with only two notable features. The first appears near 10^{15} eV as a steepening of the spectral slope from $\propto E^{-2.7}$ to $\propto E^{-3.0}$ and is called the 'knee' of the spectrum. The energy of the knee coincides roughly with the highest

[*] jjb@phys.psu.edu; phone 1 814 863 0195; Departments of Physics and of Astronomy & Astrophysics, Penn State, Box 253, 104 Davey Laboratory, University Park, PA, USA, 16802.

energies expected from shock acceleration in supernova remnants. A second feature, known as the 'ankle', appears at ~10^{19} eV and is believed to be associated with the appearance of a new and presumably extragalactic component.

Measurements of cosmic ray composition offer a means of distinguishing among models of cosmic ray origin and propagation. Nuclei differ in their charge, charge-to-mass ratio, and nucleosynthetic origin. In particular, propagation of nuclei in magnetic fields depends on the magnetic rigidity, defined as momentum per unit charge, of the particle. At a given total energy per particle, lower charge nuclei such as protons will have a larger rigidity and will thus have a larger gyroradius and sample longer length scales than nuclei such as iron. Protons will thus show evidence of the effect of the finite size of the accelerating region, believed to be responsible for limiting the maximum particle energies, at lower energies than heavy nuclei. Recent discussions of the status of studies of the knee may be found in references 1 and 2.

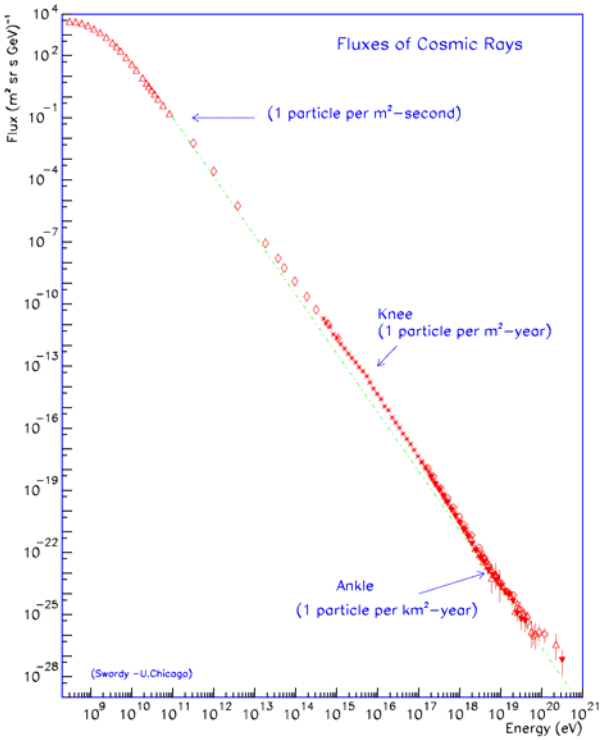

Figure 1: The cosmic ray all-particle spectrum (figure compiled by S. Swordy)

The Cosmic Ray Energetics and Mass (CREAM) balloon experiment is designed to measure cosmic ray elemental spectra from 10^{12} to 10^{15} eV (1-1000 TeV). This measurement is expected to yield information about nuclear energy spectra, and search for energy-dependent composition related to the knee. In order to collect as much data as possible, CREAM is designed to be carried aloft by NASA's new Ultra-Long Duration Balloon (ULDB), a super pressure helium balloon which can remain in the upper atmosphere (~33 km) for up to 100 days per flight. Multiple flights of CREAM will be required to extend the measured spectra to the highest possible energies. The first CREAM launch is scheduled for December 2003-January 2004 from Antarctica.

2. THE CREAM INSTRUMENT

The CREAM instrument, shown in Figure 2, consists of three major particle detectors. Particles entering the top of the instrument first cross the Timing Charge Detector (TCD), which measures the yield of light produced by the particle in plastic scintillator. The light yield is a function of the particle charge and velocity. The particles then traverse a transition radiation detector (TRD), which measures a signal which is a function of the charge and of the Lorentz factor γ of the particle.[†] The TRD provides a measure of the Lorentz factor for particles with charge greater than $3e$. The TRD is divided into two sections; between these sections a plastic Cerenkov detector is inserted. The Cerenkov detector responds only to particles with velocity exceeding the velocity of light in the plastic, and allows CREAM to reject the abundant low energy cosmic rays present in Antarctica. After leaving the TRD, particles enter the calorimeter module (Figure 4), which consists of a sampling tungsten calorimeter preceded by a carbon target. The calorimeter is used to determine the particle's energy for all nuclei, including particles with charge magnitude less than $3e$ for which the TRD cannot reliably provide an indication of the particle energy. The TRD and calorimeter have different systematic biases

[†] The Lorentz Factor is $\gamma = \left(1 - \frac{v^2}{c^2}\right)^{-\frac{1}{2}}$, where v is the particle velocity and c is the velocity of light. γ is approximately the ratio of the particle energy to its mass for the extremely relativistic particles considered here.

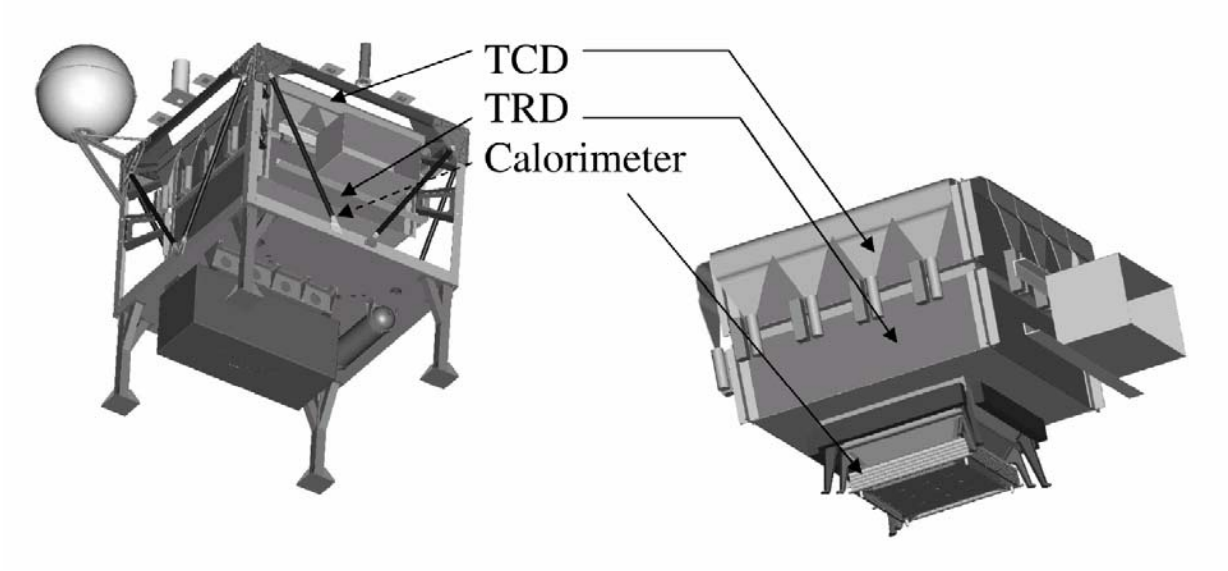

Figure 2 Schematic view of the CREAM instrument with and without its support structure

in determining the particle energy, and use of both techniques allows an in-flight intercalibration of the two techniques and thus a more reliable determination of the energy. The CREAM instrument is the first balloon payload to employ a calorimeter and TRD together in this way.

2.1 The Transition Radiation Detector

The CREAM TRD consists of two sections of three layers each of polystyrene foam radiator combined with thin-walled proportional tubes filled with a xenon gas mixture. One advantage of this design lies in not requiring an external pressure vessel, which significantly reduces the weight of the detector, an important consideration for any balloon payload. The transition radiation x-rays produced by nuclei passing through the radiators are measured to estimate both the Lorentz factor and the trajectory of the particle through the instrument. The TRD will be used to measure nuclei with an energy resolution of 15% for carbon and 7% for iron at a Lorentz factor ~3000. The energy response can be calibrated using high Lorentz factor charged particles in a test beam. The calibration can be easily scaled according to charge magnitude squared to determine the response for heavier nuclei, since the response depends only on linear electromagnetic properties of the materials and particles involved.

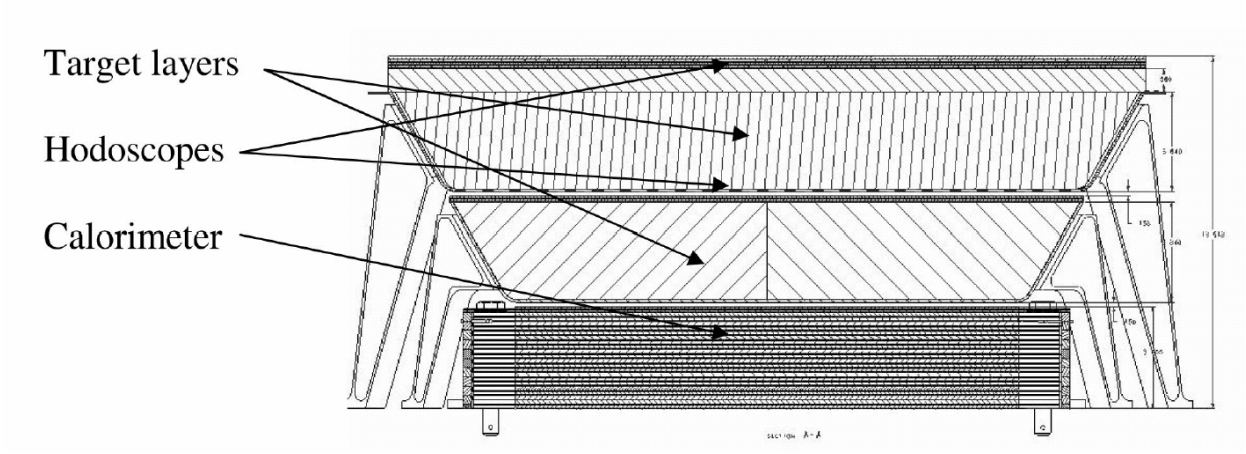

Figure 3: A schematic side view of the CREAM calorimeter module

2.2 The Calorimeter Module

The CREAM calorimeter module has two components. The first is an electromagnetic calorimeter comprised of twenty 50 cm × 50 cm tungsten plates, 3.5 mm (1 radiation length) thick, alternating with twenty layers of fifty 50 cm × 1 cm plastic scintillating fiber ribbons, 0.5 mm thick. The second is a 19 cm (0.45 interaction length) thick densified graphite trapezoidal target with an opening angle of 30° optimized for the largest effective geometry factor. The target is interleaved with a set of plastic scintillating hodoscopes above the calorimeter for tracking enhancement and supplemental charge measurements. The carbon target provides a region for the incident particles to undergo hadronic interactions while minimizing the mass of the target. The neutral pions produced in these interactions decay into energetic photons, which then produce an electromagnetic shower in the tungsten calorimeter. The energy of this shower grows with the energy of the incident particle. Additional discussion of the calorimeter can be found in reference 3.

2.3 The Ultralong Duration Balloon (ULDB) Vehicle

CREAM is scheduled to fly as the first ultralong duration balloon (ULDB) science payload. ULDB flights are a new capability being developed by NASA to allow long exposures of experiments in near-space conditions while retaining the low cost of balloon experiments compared to space flight. Balloon flights allow for recovery of instrumentation, which is especially beneficial in developing and testing new detection techniques. Balloons typically fly at altitudes of 33 to 37 kilometers, with a residual atmospheric overburden of 5 to 10 g/cm^2.

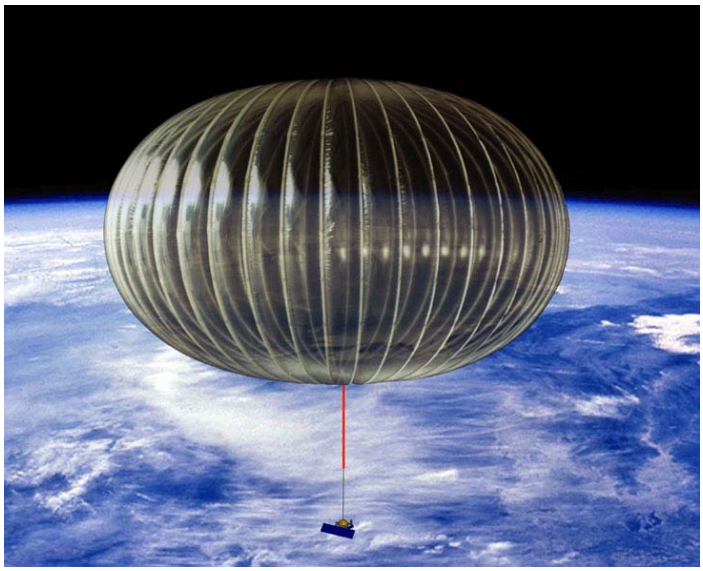

Figure 4 Artist's conception of a ULDB balloon at float

Conventional high-altitude balloons are vented 'zero-pressure' balloons using helium as the lift gas. Zero-pressure balloons are launched only partially inflated, and the helium expands to fill the balloon as the payload reaches the design float altitude. When the balloon is aloft during the daytime, the helium warms and expands and the balloon vents any helium which exceeds the volume of the balloon. At night, the helium cools and the balloon volume decreases, causing the balloon to descend. This descent is halted by dropping ballast to reduce the weight of the balloon system. Use of vented balloons limits the stress on the balloon material due to internal pressure generated by the lift gas. However, the need for ballast at each day-night transition limits the flight duration which can be achieved. Conventional flights are typically one or two days in duration when conducted in mid-latitude regions. Conventional balloons have been used in Antarctica in the austral summer circumpolar circulation to achieve flights over thirty days long with minimal ballast requirements due to the lack of day-night transitions.

In the ULDB balloon, the requirement for ballast is eliminated by sealing the helium within the balloon. However, this causes added stress in the balloon material when the helium expands during the day. The ULDB design employs a 'pumpkin' shaped design, shown in Figure 5, where the balloon material is deployed as lobes of material between vertical tendons. The reduced radius of curvature of these bulging lobes leads to a reduced stress in the balloon material for a given amount of internal overpressure in the balloon. Ultralong duration balloon flights are expected to last sixty to one hundred days. CREAM will be launched from Antarctica during the austral summer circumpolar circulation, and will be allowed to continue flying when the circulation breaks up in late summer and a more northerly trajectory may result. The Antarctic launch site was selected to minimize the chance that an early termination of the flight would be required to avoid overflight of large population centers. The ULDB balloon is now undergoing test flights, and the CREAM flight is scheduled for late 2003.

3. THE TIMING CHARGE DETECTOR

General Principles of Operation

The charge detector for CREAM must satisfy several objectives. First, it must measure charge as well as possible. The minimum requirement is identification of the five major element groups H, He, CNO, Ne-S and Ar-Ni, with identification of the individual elements a desirable aim. This must be done in the presence of a background comprised of particles generated by showers in the calorimeter. This background is most severe for interacting highest energy events seen by CREAM, which are the most interesting and rare events we will detect. These objectives must also be met in a constrained environment, which calls for a design with as low a channel count and power consumption as possible. Finally, the cost of the system is important, since recovery of the instrument is not always possible. One would like to build multiple copies of the instrument both to increase the exposure and to guard against the consequences of a delayed or impossible recovery.

The traditional approach to charge detection in the vicinity of calorimeters is use of finely segmented detectors so that the primary particle is the only particle producing a signal in a segment of the detector. The calorimeter data are used to select the pixel corresponding to the primary by pointing along the shower axis back to the charge detector. Use of this technique requires the charge detector to have pixel areas of a few square centimeters, which leads to a large channel count. The need for fine pointing also drives the design of the calorimeter.

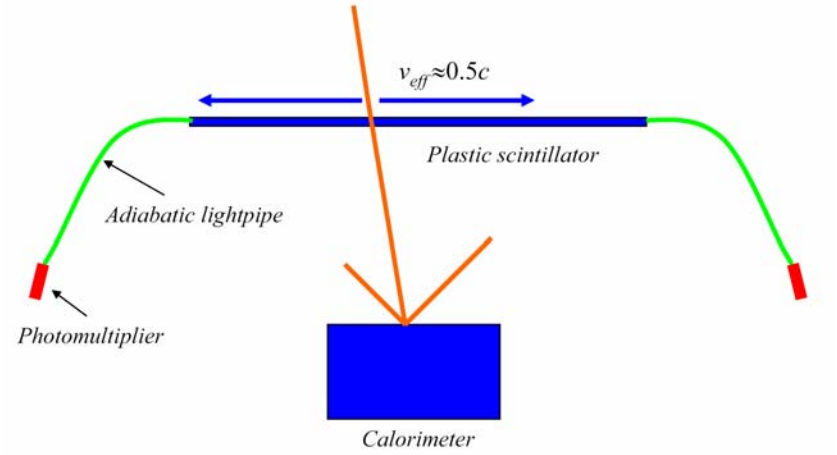

Figure 5 A schematic of the principle of the timing charge detector. The primary particle crosses the scintillator at velocity c and impacts the calorimeter, generating a signal which propagates along the scintillator at an effective velocity of 0.5*c*. This signal reaches at least one end of the scintillator before albedo particles from the calorimeter can reach the scintillator at velocity *c*.

The timing charge detector instead takes advantage of a unique property of the primary particle. Since the primary particle caused the shower, its signal is generated several nanoseconds before the shower. Albedo particles then must return to the charge detector before generating a signal. Figure 6 illustrates a detector arrangement taking advantage of this brief interval. A thin slab of plastic scintillator is coupled at both ends to adiabatic lightpipes, which are constructed to map the ends of the scintillator to the face of fast photomultiplier tubes. The adiabatic lightpipes gradually change in cross section from the narrow rectangle formed by the end of the scintillator to the round face of the photomultiplier, with the cross-sectional area of the lightpipe remaining constant. For the geometry of the CREAM instrument, there is no set of trajectories with less than 3 nanoseconds delay between the signal due to the primary particle and the earliest possible albedo particle at one active end of the detector, and for the best geometries up to 8 nanoseconds are available. By making a measurement that relies upon only the first few nanoseconds of signal observed at each photomultiplier and using reconstruction techniques derived from time-of-flight measurement it is possible to identify the signal due to the incident primary. Figure 6 shows a simulated 100 TeV proton event as seen in the time-domain at each photomultiplier face in a TCD slab. This figure illustrates both the significant amount of albedo present and the clean separation of the initial particle in the time domain.

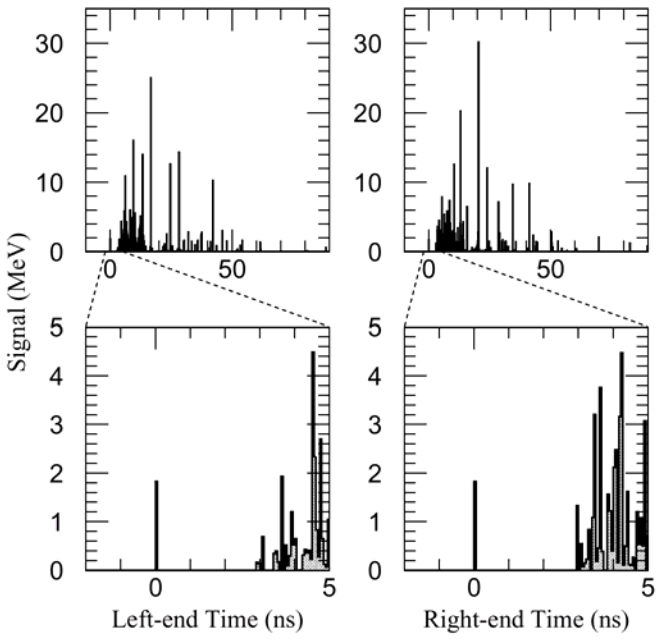

Figure 6: Simulated energy deposits in a TCD scintillator due to a 10^{14} eV cosmic ray proton and the albedo generated by the subsequent shower in the calorimeter. The time plotted for each energy deposit corresponds to the time at which the signal would be observed at the two ends of the TCD slab. The lower panels display the initial portion of the signal on an expanded timescale, showing the isolated 2 MeV pulse from the primary particle. This event corresponds to particle traversing both the TCD and calorimeter at the center, which is the worst case geometry.

Detector Description

The CREAM TCD consists of two layers of four plastic scintillator slabs each. Each scintillator slab is 1.2 m long, 0.3 m wide, and 5 mm thick. A scintillator slab module is shown in Figure 7. The scintillator used is Bicron BC-408, which is economical and has a fast response. The four scintillators in each layer are placed alongside one another to cover a 1.2 m by 1.2 m square, and the two layers are oriented with the long axes of the respective scintillators perpendicular to one another. The ends of the scintillators are glued to adiabatic lightpipes constructed from acrylic plastic containing ultraviolet absorbing additives. The ultraviolet absorption of the lightpipe plastic reduces the effect of Cerenkov emission in the lightpipes while having a negligible effect on the scintillation signal. The lightpipes bring the scintillation light to Photonis XP2020UR photomultipliers. The scintillators are wrapped in crinkled aluminum foil and the wrapping is covered with DuPont black Tedlar to render the detector light-tight. At least 100 photoelectrons are detected at each photomultiplier for a singly charged minimum ionizing particle which strikes the center of the detector

Extraction of the Charge Measurement

Fluctuations in the measurement process limit the charge resolution which can be achieved with a particular detector arrangement. For a charge detector in the CREAM detector, fluctuations due to albedo would be the dominant source of charge misidentification without special measures to eliminate their effect. Once albedo is eliminated via the timing technique or via segmentation of a detector, the dominant remaining source of fluctuations is fluctuations in the light produced in the scintillator due to fluctuations in ionization energy loss convolved with the scintillator response. For a total of 1 cm of scintillator, this results in a charge resolution of 0.2*e* at oxygen, rising to 0.35*e* at iron due to saturation of the scintillator response. Statistical fluctuations in the number of photoelectrons observed contribute 0.05*e* to the charge resolution at oxygen and about 0.09*e* at iron. This contribution is negligible when added in quadrature with the dominant energy loss fluctuations. When charge integration of the photomultiplier pulse is used, the fluctuations due to photoelectron statistics dominate the electronic contribution to the resolution. Integration of the signal cannot be used to extract the charge information from only the early portion of the signal, so in evaluating other methods of extracting the charge information one must account for the degraded resolution of the technique compared to integration.

The shape of the light pulse is independent of the charge; this implies that the slew rate of the leading edge of the pulse is proportional to the peak pulse height and to the integrated area of the pulse. The slew rate of a signal may be measured by measuring the time at which it crosses two known comparator thresholds. In practice, to measure the wide dynamic range (10^3) of pulses expected a series of eight thresholds separated by factors of about 2.5 are needed. The threshold crossing times must be measured with a resolution of 50 ps. This measurement technique provides a charge measurement adequate to resolve the elements hydrogen through silicon.

For elements beyond oxygen, the signal due to the primary particle is expected to have the highest peak value. An ultra fast peak detector sampling this peak value can thus be used to measure the charge of the primary particle. Such a peak

Figure 7: A TCD detector module being prepared for testing. The active section of detector is the long flat section. The adiabatic lightpipes make a 90º bend, and carry the light to the photomultipliers. The detector is wrapped in aluminum foil covered with DuPont Tedlar. Additional modules can be seen in the background.

detector[4] can be constructed using fast op amps and Schottky diodes which accurately captures the peak of a signal with 3 ns rise time. The resolution of a pulse peak measurement contributes about 0.1*e* to the charge resolution at oxygen and 0.17*e* to the charge resolution at iron. This is still small compared to the intrinsic resolution due to energy loss fluctuations when added in quadrature.

The CREAM readout will employ both measurements of the leading edge slew rate and of the peak of the signal, using multiple signals extracted from the anode and dynodes of the photomultipliers. Conventional integrating channels of electronics are also included to allow calibration of the system with non-interacting particles. Detectors are now in preparation for a test beam, and for integration with the CREAM TRD and calorimeter.

ACKNOWLEDGMENTS

This work has been supported through grants from the National Aeronautics and Space Administration, including grants NAG5-5248, NAG5-5249, and NAG5-5250. We also wish to acknowledge the assistance of Scott Posey and John Passeneau in the development of the timing charge detector.

REFERENCES

1. S. Yoshida. "The Cosmic Ray Measurements Above 1 TeV." in.*Proceedings of the 26th International Cosmic Ray Conference (Salt Lake City), Invited, Rapporteur, and Highlight Papers.* Edited by B.L. Dingus, D. B. Kieda, and M. H. Salamon. 1999. AIP Conference Proceedings 516.

2. S. P. Swordy *et al.* "The Composition of Cosmic Rays at the Knee." *Astroparticle Physics*, in press. (preprint available as astro-ph/0202159).

3. O. Ganel *et al*., "Cosmic Ray Energetics and Mass (CREAM):Calibrating a Cosmic Ray Calorimeter", Proceedings of the 10th International Conference on Calorimetry in Particle Physics, in press. 2002. World Scientific.

4. U. Tietze, C. Schenk, and E. Schmid.. *Electronic circuits: design and applications.* New York: Springer Verlag, 1991. (Figure 25.33)